HHS Public Access

Author manuscript

Hepatology. Author manuscript; available in PMC 2018 April 01.

Published in final edited form as:

Hepatology. 2017 April ; 65(4): 1336–1351. doi:10.1002/hep.29078.

Central Role of the TIR domain-containing adaptor-inducing interferon-β (TRIF) Adaptor Protein in Murine Sterile Liver Injury

Katherine J. Brempelis[1,2,3], **Sebastian Y. Yuen**[2], **Nicole Schwarz**[2,4], **Isaac Mohar**[2], and **Ian N. Crispe**[2]

[1]Department of Global Health, University of Washington, Seattle, WA 98195, USA

[2]Department of Pathology, University of Washington, Seattle, WA 98195, USA

[3]Ben Towne Center for Childhood Cancer Research, Seattle Children's Research Institute, Seattle, WA 98101, USA

[4]Institute of Immunology, University of Medical Centre Hamburg-Eppendorf, Martinistrasse 52, 20246 Hamburg, Germany

Abstract

Multiple pathways drive the sterile injury response in the liver; however, it is unclear how the type of cells injured or the mechanism of injury activates these pathways. Here, we use a model of selective hepatocyte death to investigate sterile liver injury. In this model, the TIR-domain-containing adaptor-inducing interferon-β (TRIF) was a central mediator of the resulting intrahepatic inflammatory response that was independent of both upstream Toll-like receptor (TLR) 4 signaling and downstream type I IFN signaling. TRIF was required for the induction of IL-10, IL-6, and IL-1β cytokines. Conversely, although the induction of CCL2 and CXCL1 chemokines and the up-regulation of chemokine (*Ccl2*, *Ccl7, Cxcl1*, *Cxcl2*, and *Cxcl10*) and cell-adhesion (*Icam1* and *Vcam1*) genes involved in myeloid cell recruitment was reduced in a majority of $TRIF^{-/-}$ mice, a subset of $TRIF^{-/-}$ mice showed breakthrough inflammation and the ability to induce these genes and proteins, indicating that redundant pathways exist to respond to hepatocyte death. Furthermore, we found that hepatocytes themselves were the main responders to hepatocyte death, increasing transcription of genes involved in myeloid cell recruitment more than either liver sinusoidal endothelial cells (LSECs) or Kupffer cells (KCs).

Conclusion—Our studies define a TRIF-dependent, TLR4- and type I IFN-independent pathway of sterile liver injury in which hepatocytes are both the targets of damage and the principal responding cell type.

Keywords

Hepatocyte; innate immunity; inflammation; TLR; TRIF

Corresponding author: Ian N. Crispe, Department of Pathology, University of Washington, 1959 NE Pacific Street, Seattle WA 98195. Phone number: 206-616-2778. crispen@uw.edu.

Disclosures: The authors declare no competing financial interests.

Tissue damage generally induces a robust sterile inflammatory response comprised of increased production of inflammatory mediators and recruitment of neutrophils and monocytes to the site of injury (1). When the sterile inflammatory response is short-lived, the tissue recovers; however, the response may also produce persistent inflammation, which in the liver, can lead to fibrosis, cirrhosis, and hepatocellular carcinoma (2, 3). Drug-induced damage (acetaminophen (APAP) hepatotoxicity), alcoholic liver steatohepatitis, diet-induced damage (non-alcoholic steatohepatitis), and mechanically-induced damage (ischemia-reperfusion injury), all promote cell death within the liver.

Damage-associated molecular patterns (DAMPs) released from dying cells signal through the same pattern recognition receptors that recognize pathogen-associated molecular patterns to initiate the inflammatory response (1). Though there are multiple families of pattern recognition receptors that bind DAMPs, TLRs are an important class of pattern recognition receptors in the sensing of sterile liver injury. Multiple mouse models of sterile inflammation have shown a central role for signaling through TLRs and their downstream effectors, TRIF and myeloid differentiation primary-response gene 88 (MyD88).

Models of sterile inflammation in the liver have provided key insights about the inflammatory pathways involved in the response to liver damage. There exists, however, a knowledge gap concerning the sterile inflammatory response to the death of each specific cell type. Models of toxic liver injury result in complexity that is challenging to analyze. For example, in APAP-mediated toxicity, injury to LSECs and disruption of the microvasculature precedes necrosis of hepatocytes, occurring as early as 30 min after drug administration (4). In concanavalin A-induced hepatitis, LSECs are eliminated early in the pathology by CD4+ T cells, destroying the lining and exposing hepatocytes to activated T cells (5). Additionally, the concanavalin A model of hepatitis relies on components of the adaptive immune system, activated T cells, to induce hepatic damage, further complicating efforts to study the response of the innate immune system (6, 7). Models of ischemia-reperfusion produce no clearer results as the death of both LSECs and hepatocytes occurs (8).

Inflammation in response to cell death is critically important in the liver not only in situations of drug-, diet-, and mechanically-induced damage, but also in the context of infection, where inflammation is complicated by responses to host cell death and pathogen. Separating the different pathways of inflammation—those against pathogen versus those against host cell death—may prove essential to address inflammatory liver disease. In particular, the response to hepatocyte death is critical to understand as it is a central component of both damage induced by infectious and non-infectious insults.

We have, therefore, developed a mouse model to study sterile liver inflammation initiated by hepatocyte-specific death. We found that TRIF, independent of TLR4 and type I IFN signaling, plays a key role in the initiation of sterile inflammation, of which hepatocytes themselves are major regulators.

Materials and Methods

Mice

Experiments used male mice, aged 8–12 weeks. C57BL/6J, C57BL/6NJ, TLR3-deficient ($TLR3^{-/-}$), TLR4-deficient ($TLR4^{-/-}$), and MyD88-deficient ($MyD88^{-/-}$) mice were purchased from the Jackson Laboratory (Bar Harbor, ME). IFN (α and β) receptor 1-deficient $(IFNAR1)^{-/-}$ and TRIF-deficient ($TRIF^{-/-}$) breeders were a gift from Dr. Alan Aderem (University of Washington/Center for Infectious Disease Research) and used to breed experimental mice in-house at the University of Washington. Receptor-interacting protein kinase 3-deficient ($RIPK3^{-/-}$) mice were a gift from Dr. Andrew Oberst (University of Washington). All mouse experiments described in this study were performed under Institutional Animal Care and Use Committee approval (University of Washington, protocols #4308-01 and #4308-02). They were housed in a specific pathogen-free environment, provided with *ad libitum* food and water unless otherwise noted, and monitored daily.

Model of hepatocyte-specific death

Male mice aged 8–12 weeks were retro-orbitally injected with 5×10^9 DNase-resistant genomes (DRGs) of rAAV8.mCherry.T2A.hDTR (rAAV, recombinant adeno-associated vector; hDTR, human diphtheria toxin receptor). After allowing two weeks for vector expression, mice were injected intraperitoneally with either 20 ng diphtheria toxin (DT) (Sigma-Aldrich, St. Louis, MO) in 200 μL 1X PBS or with 200 μL 1X PBS. Mice were anesthetized for liver perfusion at approximately 6, 12, 24, 28, 72, and 96 hours post DT injection. Livers were perfused as previously described with slight modifications, noted in the Supporting Materials and Methods (9).

Other Materials and Methods

Additional materials and methods are described in the Supporting Materials and Methods.

Results

Model of hepatocyte-specific death

To identify pathways of sterile inflammation in the liver we developed a mouse model of hepatocyte-specific death. We designed an rAAV vector encoding the fluorescent reporter protein mCherry and the hDTR, rAAV8.pAlb.mCherry.hDTR (Figure 1A). This vector uses the AAV serotype-8 capsid proteins to preferentially target to the liver (Figure 1B) and the mouse α-fetoprotein enhancer in combination with the albumin promoter for hepatocyte-specific expression of transgenes (Figure 1C–D). Mice received 5×10^9 DRGs of vector by retro-orbital injection. After allowing two weeks for vector expression to stabilize within the mouse, we induced hepatocyte death by injection of DT. Liver damage, measured by ALT levels, peaked at 48 hours (Figure 1E).

Histological examination showed the presence of a cellular infiltrate as well as extensive hepatocyte necrosis by 48 hours (Figure 1F). Hepatocytes undergoing mitosis, indicative of tissue repair, appeared by 48 hours (arrow, Figure 1F). By 72 hours, the infiltrate had increased and there were increased numbers of mitotic hepatocytes, indicating further tissue

repair, though there still remained evidence of dying hepatocytes. Immunofluorescence showed strong and diffuse mCherry expression limited to the cytoplasm of hepatocytes in the control group. By 24 hours and continuing to 48 hours post DT administration, the mCherry signal was consolidating into round vacuoles largely within the cytoplasm of hepatocytes but also within cells in the sinusoids. By 72 hours, large vacuoles of mCherry signal were less concentrated in hepatocytes, with smaller puncta of mCherry signal appearing throughout the cytoplasm of hepatocytes and within cells in the sinusoids. Taken together, these observations suggest the occurrence of either autophagy within dying cells or phagocytosis of dying cells by hepatocytes and other non-parenchymal cells within the liver. To investigate further the mechanism of DT-induced hepatocyte death, we used a Huh7 hepatoma cell line that stably expresses TLR3 (Huh7-TLR3) as well as RIPK3$^{-/-}$ mice. These analyses suggest DT kills hepatocytes in a caspase 3/7-independent, non-necroptic manner (Supporting Figure 1).

To assess whether our hepatocyte-targeted model of acute liver injury aligned with a more physiological, but less-targeted model, such as APAP-induced liver injury, we measured a broad panel of transcriptional changes in response to both mechanisms of damage. Analysis of cellular infiltrate and gene expression indicated that both models produce similar changes in gene expression at peak injury (Supporting Figure 2), suggesting that our model of hepatocyte-specific death may allow us to resolve mechanisms of injury that are potentially obscured in a more complex context.

Neutrophils and monocytes are recruited to the liver following hepatocyte death but do not contribute to liver injury

Sterile inflammation, and APAP-induced liver injury in particular, is characterized by a neutrophil and monocyte infiltrate (10, 11). To determine if monocytes and neutrophils infiltrated the liver in response to hepatocyte death, we used flow cytometry to assess the populations present in the liver in control mice and at 6, 12, 24, 48, 72, and 96 hours after injection of DT. Following doublet exclusion and size gating (Supporting Figure 3), we gated for LSECs, KCs, neutrophils, eosinophils, and monocytes—further split into Ly6C^{hi} and Ly6C^{lo} populations, and further characterized based on their expression of CD11c and MHC-II (I-A/I-E) (Figure 2A, control; and 2B, 48 hours). Neutrophils began infiltrating the liver 12 hours following DT injection and peaked between 24–48 hours while monocytes began infiltrating the liver by 24 hours and peaked between 48–72 hours (Figure 2C). Within the monocyte population, the proportion of Ly6C^{hi} monocytes began to increase by 24 hours while the proportion of Ly6C^{lo} monocytes began to increase by 48 hours (Figure 2C).

Several studies suggest that neutrophils and/or monocytes may contribute to damage in APAP liver injury models (12). This led us to ask whether monocytes or neutrophils contributed to peak liver injury following hepatocyte death. To address this question, we used anti-CCR2 and anti-Ly6G antibody to deplete monocytes and neutrophils, respectively, prior to, during, and following the administration of DT (Supporting Figures 4A and 5A). Antibody-mediated depletion of monocytes reduced the number of monocytes in the liver without affecting the number of neutrophils (Supporting Figure 4B–D) and antibody-mediated depletion of neutrophils reduced the number of neutrophils in the liver without

affecting the number of monocytes (Supporting Figure 5B–D). Forty-eight hours following DT administration, neither monocyte-depleted nor neutrophil-depleted mice showed a difference in ALT levels compared to control mice (Supporting Figures 4E and 5E), indicating that monocytes and neutrophils are not mediators of peak liver injury. This does not rule out the possibility that monocytes and/or neutrophils contribute to liver injury either before or after peak injury.

The induction of genes involved in monocyte and neutrophil recruitment is strongest in hepatocytes

The presence of neutrophils and monocytes caused us to ask whether chemokines and adhesion molecules involved in myeloid cell recruitment were induced as a component of the inflammatory response against hepatocyte death. To examine this, we looked at the expression of chemokine genes in total liver, hepatocytes, LSECs, and KCs 6, 12, 24, 48, 72, and 96 hours following DT administration. Genes for monocyte-recruiting chemokines (*Ccl2*, *Ccl5, Ccl7*, *Cxcl10*), neutrophil-recruiting chemokines (*Cxcl1*, *Cxcl2*), and adhesion molecules (*Icam1*, *Vcam1*) were strongly induced across all populations (Figure 3A). For *Ccl7* expression in hepatocytes, levels of transcript were not detectable in 3 of 4 control mice; however, *Ccl7* transcript levels were induced by 12 hours and increased by 24 hours in hepatocytes (Figure 3B). Induction was greatest in the hepatocytes for almost all genes measured and peaked at 24 hours. Examination of the relative expression levels between hepatocytes, LSECs, and KCs revealed that KCs generally expressed the highest levels of transcript in control mice, with the notable exception that hepatocytes expressed the most *Cxcl1* (Figure 3B). Upon hepatocyte death, however, hepatocytes increased the level of gene expression for *Ccl2*, *Cxcl2*, *Cxcl10*, and *Icam1* so that it surpassed that of LSECs and KCs, further suggesting that hepatocytes are the central responding cell (Figure 3B).

The immune response following hepatocyte death is TRIF-dependent but TLR4- and type I IFN-independent

The cytokine profile suggested the involvement of type I IFN signaling which has been shown to induce *Ccl2* in mouse models of liver inflammation (13). Gene expression analysis indicated that *Ifn-beta* (*Ifnb1*), the main downstream effector of TRIF, was strongly induced in total liver 24 hours following liver injury, while transcripts driven by MyD88-dependent signaling showed more modest induction (Supporting Figure 6). The preferential induction of *Ifnb1* over MyD88-driven cytokines indicated that the inflammation could be controlled by TRIF-dependent, IFN-dependent signaling. To address this, we induced hepatocyte death in TRIF$^{-/-}$ and MyD88$^{-/-}$ mice and measured the response at 48 hours, the time point when ALT levels peaked in the time course. Both TRIF$^{-/-}$ and MyD88$^{-/-}$ mice showed significantly reduced elevation in ALT and neutrophil infiltrate compared to wild type mice (Figures 4A and 4C); however, only TRIF$^{-/-}$ mice showed a significant reduction in the influx of monocytes (Figure 4B). While we found that the influx of neutrophils required MyD88, MyD88$^{-/-}$ mice were only partially protected from liver damage, further suggesting that neutrophils do not play a role in liver damage. Overall, the magnitude of the effects on the ALT and monocyte levels was more dramatic in the case of TRIF$^{-/-}$ mice.

The literature indicates that signaling via TRIF activates interferon regulatory factor 3, which drives expression of type I IFN, and particularly of IFN-β (14). The large induction of *Ifnb1* suggested to us that type I IFN signaling may be driving inflammation downstream of TRIF-mediated signaling. To test this, we induced hepatocyte death in IFNAR1$^{-/-}$ mice and measured the response 48 hours after DT administration. IFNAR1$^{-/-}$ mice responded to hepatocyte death with the same increases in ALT, neutrophil infiltrate, and monocyte infiltrate as wild type mice (Figure 4A–C), suggesting that type I IFN signaling following hepatocyte death does not propagate liver damage despite the upregulation of *Ifnb1* in total liver.

Finally, to ask which receptor was responsible for initiating the inflammation to hepatocyte death, we examined the response to hepatocyte death in TLR4$^{-/-}$ and TLR3$^{-/-}$ mice at 48 hours following DT administration, as TRIF is the common signaling adaptor for TLR3 and TLR4 (15). ALT levels, neutrophil infiltrate, and monocyte infiltrate were induced to comparable levels in wild type and TLR4$^{-/-}$ mice (Figure 4A–C). Although this suggests that TLR3 is the DAMP receptor, we were unable to test this decisively, since the TLR3$^{-/-}$ mice were not transduced to equal levels by the rAAV8.mCherry.hDTR vector. Therefore, although we obtained very low ALT levels in DT-treated, vector-transduced TLR3$^{-/-}$ mice, this result could not be interpreted (data not shown). Preliminary studies using the Huh7 hepatoma cell line, which lacks TLR3, show that a subset of the genes up-regulated in wild type mice following DT-induced death are also up-regulated in the Huh7 cells, suggesting that TLR3 may not be required for this TRIF-dependent signaling pathway (Supporting Figure 7).

Absence of TRIF results in reduced production of myeloid cell-recruiting factors, except in mice exhibiting breakthrough inflammation

Since TRIF$^{-/-}$ mice exhibited reduced monocyte and neutrophil infiltrate, we next asked if the up-regulation of monocyte- and neutrophil-recruiting genes was also impaired in TRIF$^{-/-}$ mice. At 48 hours following injection of DT, TRIF$^{-/-}$ mice showed less induction of *Ccl2*, *Ccl5*, *Ccl7*, *Cxcl1*, *Cxcl2*, *Cxcl10*, *Icam1*, and *Vcam1* transcripts in total liver when compared to wild type mice; and though not statistically significant for all transcripts, these transcripts also trended towards reduction in hepatocytes (Figures 5A and 5C). Examination of serum for CCL2 and CXCL1 revealed that both chemokines were significantly reduced in TRIF$^{-/-}$ mice compared to wild type mice (Figure 5D).

While TRIF deficiency resulted in reduced inflammation in a majority of mice as measured by ALT levels, cellular infiltrate, mRNA levels, and protein levels, we observed a subset of TRIF$^{-/-}$ mice that appeared to experience breakthrough inflammation. We hypothesized that total liver mRNA and serum protein levels would increase with increasing liver injury in the TRIF$^{-/-}$ mice. To test this hypothesis, we correlated cellular infiltrate, total liver mRNA, and serum protein levels to serum ALT levels in DT-treated TRIF$^{-/-}$ and wild type mice. We found that *Ccl2*, *Ccl7*, *Cxcl1*, *Cxcl10*, *Icam1*, and *Vcam1* mRNA and CCL2 and CXCL2 protein were significantly correlated with ALT and that often the correlation was stronger in TRIF$^{-/-}$ than in wild type mice (Figures 5B and 5E). These findings suggest that an alternate mechanism or mediator of inflammation, such as MyD88, compensates for the lack of TRIF

in a subset of mice. Monocyte infiltrate correlated with increasing ALT, however, neutrophil infiltrate was not significantly correlated with increasing ALT levels (Figure 5F). The lack of neutrophil correlation with ALT level could be a result of measuring at 48 hours rather than an earlier time point, as we found neutrophils to begin infiltrating the liver earlier than monocytes (Figure 2B).

TRIF is required for increased production of IL-1β, IL-10, and IL6

The inflammatory cytokines TNF-α, IL-1β, and IL-6 and the anti-inflammatory cytokine IL-10, are commonly produced in response to acute liver injury (10). We evaluated the levels of these cytokines in serum from wild type mice and TRIF$^{-/-}$ mice 48 hours following DT injection. The production of IL-10, IL-6, IL-1β, and TNF-α was reduced in TRIF$^{-/-}$ mice compared to wild type mice 48 hours following DT injection (Figure 6A). Correlation of cytokine and ALT levels in serum from DT-treated mice demonstrated that while TNF-α correlated weakly, IL-10, IL-6, and IL-1β did not correlate with increasing liver injury in TRIF$^{-/-}$ mice (Figure 6B). This suggests that the production of IL-10, IL-6, and IL-1β following hepatocyte death requires TRIF, while the induction of TNF-α follows the same pattern as the myeloid cell-recruiting factors.

Discussion

Hepatocyte death is a key component of both pathogen- and sterile injury-induced pathologies, and contributes to the development of chronic liver disease. The inflammatory circuits that respond to host death and pathogen insult overlap extensively and models of sterile inflammation help to isolate the signaling pathways involved by removing the responses to pathogen. Though there are many mouse models of sterile liver injury, there is a lack of models to identify pathways unique to the response initiated by DAMPs released from dying hepatocytes.

We developed a mouse model of hepatocyte-specific death using an rAAV8 vector to target the hDTR construct to hepatocytes for expression. rAAV8 vectors, containing AAV2 serotype DNA and AAV8 serotype capsid proteins, are optimized for delivery of transgenes to hepatocytes. Unlike rAAV2 vectors which achieve transduction of only ~10% of hepatocytes even at high doses, rAAV8 is more efficient at transducing hepatocytes and can transduce up to 100% of hepatocytes (16). Examination of the expression pattern of *hDTR* mRNA confirmed that our rAAV8 vector provided liver- and hepatocyte-specific expression. In stark contrast to adenoviral vectors, the immune response to single-stranded AAV vectors is transient and mild, resolving within 6 hours following AAV injection (17). The response is driven by TLR9- and MyD88-dependent signaling and results in a short-term increase of infiltrating neutrophils and CD11b^{+} cells and an increase in mRNA for *Tnf*, *Ccl2*, *Ccl4*, *Ccl5*, *Cxcl2*, and *Cxcl10* (17). To assure that the initial immune response to rAAV was no longer present and that transgene expression was stable, we allowed for 2 weeks between rAAV injection and injection of DT.

Hepatocyte death, induced by injection of DT, resulted in maximal liver damage 48 hours following DT injection and was accompanied by an increase in mRNA and protein for inflammatory mediators. This response was largely dependent upon TRIF and, to a lesser

extent, also dependent on MyD88. Perhaps the most-studied liver injury driven by TRIF-dependent signaling is alcohol toxicity, where increased translocation of endotoxin from gut microbiota into the liver via the portal vein results in signaling via TLR4 in a MyD88-independent, TRIF-dependent manner (18–21). The role for TRIF signaling in other liver injury is less clear. In APAP-induced injury, TLR4 and TLR9 have been identified as key receptors involved in the recruitment of infiltrating monocytes and neutrophils and the production of IL-6, TNF-α, and IL-1β; however, the downstream signaling pathways need to be elucidated (22–25). The similarities in the inflammation profile between our model and the APAP model suggest that TRIF signaling could be important for the induction of inflammation in APAP hepatotoxicity. In a model of ischemia-reperfusion injury, TLR4$^{-/-}$ mice were protected from injury, producing less *Cxcl10*, *Icam1*, *Tnf*, *Il1b*, and *Ifng* (26). Furthermore, Zhai et al. reported that the DAMP high mobility group box 1 protein (HMGB1) signaled via a MyD88-independent, interferon regulatory factor 3-dependent route to propagate inflammation in ischemia-reperfusion injury (27). Both of these studies suggest that TRIF may be the adaptor mediating the inflammatory responses. It should be noted that signaling via TRIF generally results in production of type I IFNs (14). In sterile inflammation resulting from ischemia-reperfusion injury, IFNAR1-deficient mice were protected from liver damage and produced less transcript for *Tnf*, *Il1b*, *Il6*, *Ccl2*, *Cxcl10*, and *Icam1*, as well as had fewer infiltrating neutrophils and macrophages (28). While we observed the induction of *Ifnb1* transcript following injury, liver damage in IFNAR1$^{-/-}$ mice was not significantly different from that seen in wild type mice, eliminating a role for type I IFN signaling in the pathology of hepatocyte-specific death.

Although the models discussed above are heavily dependent upon signaling through TLR4, we find that the TRIF-dependent response to hepatocyte death is independent of TLR4. In the absence of upstream signaling through TLR4, TRIF signaling is thought to be initiated via TLR3. The role of TLR3 in sterile liver injury remains relatively unknown, though studies show it contributes to liver damage in models of APAP hepatotoxicity and concanavalin A-induced hepatitis (29, 30). As we observed ~30-fold less transduction of hepatocytes by rAAV8.mCherry.hDTR in TLR3$^{-/-}$ mice when compared to wild type mice, we could not evaluate the *in vivo* role of TLR3 signaling. It is possible that the lack of functional TLR3 in TLR3$^{-/-}$ mice either directly affects the alternative nuclear factor kB pathway, or affects the ability of rAAV to use this pathway for transgene expression as Jayandharan et al. demonstrated that the alternative nuclear factor kB pathway was necessary for the expression of AAV-encoded transgenes (31). *In vitro* studies which show that mRNA from necrotic cells signals via a TLR3- and TRIF-dependent pathway in dendritic cells support the possibility that TLR3 is the receptor responding to cell death (32). In contrast, Zhang et al. have shown that members of the DExD/H-box helicase family—DDX1, DDX21, and DHX36—signal via TRIF to induce type I IFN in response to dsRNA (33); and, the DDX21-, TRIF-dependent signaling pathway has been shown to play a role in Influenza A infection (34). Our initial studies in Huh7 human hepatoma cells indicate that the induction of certain inflammatory genes observed in our mouse model of hepatocyte-specific death are preserved in a system lacking TLR3 signaling, supporting a possible role for a TLR3-independent, TRIF-dependent inflammatory pathway.

The role hepatocytes play in sterile liver inflammation, and particularly in the response to hepatocyte death, is relatively unknown. Though limited data are available concerning the role of hepatocytes as drivers of an inflammatory response, *in vitro* studies have produced some provocative results. Primary mouse hepatocytes secrete IL-6 in response to free fatty acids and IL-17 (35) and IL-6 and TNF-α in response to free fatty acids alone (36). In mouse models of chronic injury induced by carbon tetrachloride, CCL20 was detected in hepatocytes by immunohistochemistry (37) and secreted by murine primary hepatocytes in culture (38). Additionally, hepatocytes isolated from ethanol treated mice expressed more *Cxcl1* than those from control mice (39). In our model of hepatocyte-specific death, the up-regulation of *Ccl2*, *Ccl5*, *Ccl7*, *Cxcl1*, *Cxcl2*, *Cxcl10*, *Icam1*, and *Vcam1* was greater in hepatocytes than in either LSECs or KCs, highlighting hepatocytes as key players in the sterile inflammatory response to hepatocyte death.

A number of studies have shown that cells undergoing apoptosis, necrosis, or necroptosis maintain the capacity to up-regulate transcription and protein production (40–44). IL-6 can be secreted by necrotic cells (42); IL-6, CCL2, and CXCL1 secreted by apoptotic cells (43); and most recently, necroptotic cells showed increased transcription of many genes, including *Cxcl1*, *Cxcl10*, *Ccl2*, C*cl7*, and *Il6* (44). Given the transcript repertoire we detected in our studies it is possible that dying hepatocytes are producing chemokines in our model (Figure 7A). Alternatively, or in parallel, live hepatocytes responding to mediators produced by KCs and LSECs or sensing and responding to hepatocyte death themselves—possibly through the induction of their own death—may also be responsible for the up-regulation of these transcripts (Figure 7B–7C). This latter possibility is supported by our observation that many of these transcripts are up-regulated in KCs and LSECs 6 hours following DT injection, indicating the induction of an innate immune response in neighboring cells. Finally, sensing and response by live hepatocytes is also supported by *in vitro* findings in which primary mouse hepatocytes, independent of death, increased expression for a number of inflammatory proteins including: *Cxcl1*, *Cxcl2*, *Cxcl10*, *Ccl2*, *Ccl7*, *Ccl20*, *Icam1*, *Vcam1*, *Il1b*, and *Il10* in response to bile acids (45). The results of our *in vivo* study of hepatocyte death combined with the *in vitro* study provide compelling evidence for a common inflammatory pathway induced in hepatocytes in response to insult, in these cases, DAMPs released from other dying hepatocytes or bile acids.

Interestingly, though we found that TRIF is the master regulator of inflammation induced by hepatocyte death, we observed breakthrough inflammation and sterile injury in a subset of TRIF$^{-/-}$ mice. This suggests that there are redundant pathways primed to respond to liver injury, and hepatocyte death in particular. MyD88 is a clear candidate for an alternative regulator as we saw only a partial reduction in liver injury and inflammation in MyD88$^{-/-}$ mice. We speculate that in a subset of mice, the balance between the TRIF and MyD88 signaling pathways is tipped, so that the MyD88 signaling pathway is able to drive the induction of transcripts for chemokines and cell adhesion molecules. Accordingly, studies in TRIF x MyD88 double knockout mice would elucidate whether MyD88 is able to compensate for lack of TRIF signaling.

Finally, similar to other mouse models of sterile injury, we observed an influx of neutrophils followed by an influx of monocytes to the site of injury. Our studies indicated that

monocytes and neutrophils were not driving peak liver injury; however, this does not rule out a role for either population in earlier injury or later resolution. Models of acute and chronic liver injury have demonstrated complex roles for monocytes in the induction of early injury and fibrosis to the resolution of injury (46). Most recently, $CCR2^{+}$ monocytes have been implicated in early stages of APAP-induced liver injury, while earlier studies indicate that infiltrating monocytes may play a role in the resolution of liver injury (47, 48). In our model, we initially see higher proportions of $Ly6C^{hi}$ monocytes, but by 72 hours, we see higher proportions of $Ly6C^{lo}$ monocytes. In conjunction with the histology that indicates hepatocytes are regenerating by 72 hours, it is possible that $Ly6C^{hi}$ monocytes infiltrate the liver and differentiate into $Ly6C^{lo}$ monocyte-derived macrophages which contribute to tissue repair (Figure 7D–E). This possibility is supported by two elegant studies which demonstrate the plasticity of monocytes and the ability of $Ly6C^{hi}$ monocytes to infiltrate the liver following injury and differentiate into $Ly6C^{lo}$ monocyte-derived macrophages that are important for injury resolution and tissue repair (49, 50).

In summary, we have identified TRIF as a central mediator in the response to hepatocyte-specific death. Hepatocytes themselves produce the most robust response to hepatocyte death through the up-regulation of genes for myeloid cell-recruiting factors. In serum as a whole, we see an increase in IL-6, IL-1β, and IL-10, which is absent in $TRIF^{-/-}$ mice, indicating a complete dependence on TRIF signaling for the production of these inflammatory cytokines. Conversely, although the increased expression of chemokine and cell adhesion genes and proteins associated with the myeloid cell-recruiting response was reduced in a majority of $TRIF^{-/-}$ mice, a subset of mice was able to compensate for the lack of TRIF and induce expression of this set of factors, indicating a potential redundancy for this pathway. Finally, we find the TRIF-driven response to hepatocyte death to be independent of TLR4 and type I IFN. The relevance of these finding to human liver injury is emphasized both because parallel effects are seen in APAP toxicity, an important cause of acute liver failure, and because human Huh7 cells respond to DT-induced death by inducing many of the same genes as do mouse hepatocytes.

Supplementary Material

Refer to Web version on PubMed Central for supplementary material.

Acknowledgments

Financial Support: The work was supported by NIH grants R01AI114630 and R21AI099872 to INC, and F31AA021309 to KJB.

The authors thank the University of Washington's Department of Comparative Medicine and the Vivarium staff for animal husbandry. The authors also thank the University of Washington Histology and Imaging Core for preparation of histology samples and the University of Washington Pathology Flow Core, and particularly Donna Prunkard, for assistance with cell sorting. Lastly, the authors thank Dr. Kyle Minch for sharing his expertise in microscopy and image analysis.

Abbreviations

TRIF	TIR-domain-containing adaptor-inducing interferon-β

TLR	Toll-like receptor
LSEC	liver sinusoidal endothelial cell
KC	Kupffer cell
APAP	acetaminophen
DAMPs	damage-associated molecular patterns
MyD88	myeloid differentiation primary response gene 88
DRGs	DNAse-resistant genomes
IFNAR1	interferon (alpha and beta) receptor 1
rAAV	recombinant adeno-associated virus
hDTR	human diphtheria toxin receptor
DT	diphtheria toxin

References

Authors names in bold designate shared co-first authorship.

1. Chen GY, Nunez G. Sterile inflammation: sensing and reacting to damage. Nat Rev Immunol. 2010; 10:826–837. [PubMed: 21088683]
2. Aoyama T, Paik YH, Seki E. Toll-like receptor signaling and liver fibrosis. Gastroenterol Res Pract. 2010; 2010
3. Roh YS, Seki E. Toll-like receptors in alcoholic liver disease, non-alcoholic steatohepatitis and carcinogenesis. J Gastroenterol Hepatol. 2013; 28(Suppl 1):38–42.
4. Ito Y, Bethea NW, Abril ER, McCuskey RS. Early hepatic microvascular injury in response to acetaminophen toxicity. Microcirculation. 2003; 10:391–400. [PubMed: 14557822]
5. Knolle PA, Gerken G, Loser E, Dienes HP, Gantner F, Tiegs G, Meyer zum Buschenfelde KH, et al. Role of sinusoidal endothelial cells of the liver in concanavalin A-induced hepatic injury in mice. Hepatology. 1996; 24:824–829. [PubMed: 8855184]
6. Tiegs G, Hentschel J, Wendel A. A T cell-dependent experimental liver injury in mice inducible by concanavalin A. J Clin Invest. 1992; 90:196–203. [PubMed: 1634608]
7. Watanabe Y, Morita M, Akaike T. Concanavalin A induces perforin-mediated but not Fas-mediated hepatic injury. Hepatology. 1996; 24:702–710. [PubMed: 8781346]
8. Datta G, Fuller BJ, Davidson BR. Molecular mechanisms of liver ischemia reperfusion injury: insights from transgenic knockout models. World J Gastroenterol. 2013; 19:1683–1698. [PubMed: 23555157]
9. Mohar I, Brempelis KJ, Murray SA, Ebrahimkhani MR, Crispe IN. Isolation of Non-parenchymal Cells from the Mouse Liver. Methods Mol Biol. 2015; 1325:3–17. [PubMed: 26450375]
10. Zimmermann HW, Trautwein C, Tacke F. Functional role of monocytes and macrophages for the inflammatory response in acute liver injury. Front Physiol. 2012; 3:56. [PubMed: 23091461]
11. Liaskou E, Wilson DV, Oo YH. Innate immune cells in liver inflammation. Mediators Inflamm. 2012; 2012:949157. [PubMed: 22933833]
12. Krenkel O, Mossanen JC, Tacke F. Immune mechanisms in acetaminophen-induced acute liver failure. Hepatobiliary Surg Nutr. 2014; 3:331–343. [PubMed: 25568858]
13. Hokeness KL, Kuziel WA, Biron CA, Salazar-Mather TP. Monocyte chemoattractant protein-1 and CCR2 interactions are required for IFN-alpha/beta-induced inflammatory responses and antiviral defense in liver. J Immunol. 2005; 174:1549–1556. [PubMed: 15661915]

14. Sato S, Sugiyama M, Yamamoto M, Watanabe Y, Kawai T, Takeda K, Akira S. Toll/IL-1 Receptor Domain-Containing Adaptor Inducing IFN-β (TRIF) Associates with TNF Receptor-Associated Factor 6 and TANK-Binding Kinase 1, and Activates Two Distinct Transcription Factors, NF-κB and IFN-Regulatory Factor-3, in the Toll-Like Receptor Signaling. The Journal of Immunology. 2003; 171:4304–4310. [PubMed: 14530355]
15. Yamamoto M, Sato S, Hemmi H, Hoshino K, Kaisho T, Sanjo H, Takeuchi O, et al. Role of adaptor TRIF in the MyD88-independent toll-like receptor signaling pathway. Science. 2003; 301:640–643. [PubMed: 12855817]
16. Nakai H, Fuess S, Storm TA, Muramatsu S, Nara Y, Kay MA. Unrestricted hepatocyte transduction with adeno-associated virus serotype 8 vectors in mice. J Virol. 2005; 79:214–224. [PubMed: 15596817]
17. Zaiss AK, Liu Q, Bowen GP, Wong NCW, Bartlett JS, Muruve DA. Differential Activation of Innate Immune Responses by Adenovirus and Adeno-Associated Virus Vectors. Journal of Virology. 2002; 76:4580–4590. [PubMed: 11932423]
18. Hritz I, Mandrekar P, Velayudham A, Catalano D, Dolganiuc A, Kodys K, Kurt-Jones E, et al. The critical role of toll-like receptor (TLR) 4 in alcoholic liver disease is independent of the common TLR adapter MyD88. Hepatology. 2008; 48:1224–1231. [PubMed: 18792393]
19. Zhao XJ, Dong Q, Bindas J, Piganelli JD, Magill A, Reiser J, Kolls JK. TRIF and IRF-3 binding to the TNF promoter results in macrophage TNF dysregulation and steatosis induced by chronic ethanol. J Immunol. 2008; 181:3049–3056. [PubMed: 18713975]
20. Nanji AA, Khettry U, Sadrzadeh SM, Yamanaka T. Severity of liver injury in experimental alcoholic liver disease. Correlation with plasma endotoxin, prostaglandin E2, leukotriene B4, and thromboxane B2. Am J Pathol. 1993; 142:367–373. [PubMed: 8382006]
21. Uesugi T, Froh M, Arteel GE, Bradford BU, Thurman RG. Toll-like receptor 4 is involved in the mechanism of early alcohol-induced liver injury in mice. Hepatology. 2001; 34:101–108. [PubMed: 11431739]
22. Shah N, Montes de Oca M, Jover-Cobos M, Tanamoto K, Muroi M, Sugiyama K, Davies NA, et al. Role of toll-like receptor 4 in mediating multiorgan dysfunction in mice with acetaminophen induced acute liver failure. Liver Transpl. 2013; 19:751–761. [PubMed: 23554142]
23. Yohe HC, O'Hara KA, Hunt JA, Kitzmiller TJ, Wood SG, Bement JL, Bement WJ, et al. Involvement of Toll-like receptor 4 in acetaminophen hepatotoxicity. Am J Physiol Gastrointest Liver Physiol. 2006; 290:G1269–1279. [PubMed: 16439473]
24. Fisher JE, McKenzie TJ, Lillegard JB, Yu Y, Juskewitch JE, Nedredal GI, Brunn GJ, et al. Role of Kupffer cells and toll-like receptor 4 in acetaminophen-induced acute liver failure. J Surg Res. 2013; 180:147–155. [PubMed: 23260383]
25. Imaeda AB, Watanabe A, Sohail MA, Mahmood S, Mohamadnejad M, Sutterwala FS, Flavell RA, et al. Acetaminophen-induced hepatotoxicity in mice is dependent on Tlr9 and the Nalp3 inflammasome. J Clin Invest. 2009; 119:305–314. [PubMed: 19164858]
26. Shen XD, Ke B, Zhai Y, Gao F, Tsuchihashi S, Lassman CR, Busuttil RW, et al. Absence of toll-like receptor 4 (TLR4) signaling in the donor organ reduces ischemia and reperfusion injury in a murine liver transplantation model. Liver Transpl. 2007; 13:1435–1443. [PubMed: 17902130]
27. Zhai Y, Shen XD, O'Connell R, Gao F, Lassman C, Busuttil RW, Cheng G, et al. Cutting edge: TLR4 activation mediates liver ischemia/reperfusion inflammatory response via IFN regulatory factor 3-dependent MyD88-independent pathway. J Immunol. 2004; 173:7115–7119. [PubMed: 15585830]
28. Shen XD, Ke B, Ji H, Gao F, Freitas MC, Chang WW, Lee C, et al. Disruption of Type-I IFN pathway ameliorates preservation damage in mouse orthotopic liver transplantation via HO-1 dependent mechanism. Am J Transplant. 2012; 12:1730–1739. [PubMed: 22429450]
29. Cavassani KA, Moreira AP, Habiel D, Ito T, Coelho AL, Allen RM, Hu B, et al. Toll like receptor 3 plays a critical role in the progression and severity of acetaminophen-induced hepatotoxicity. PLoS One. 2013; 8:e65899. [PubMed: 23762449]
30. Xiao X, Zhao P, Rodriguez-Pinto D, Qi D, Henegariu O, Alexopoulou L, Flavell RA, et al. Inflammatory regulation by TLR3 in acute hepatitis. J Immunol. 2009; 183:3712–3719. [PubMed: 19710451]

31. Jayandharan GR, Aslanidi G, Martino AT, Jahn SC, Perrin GQ, Herzog RW, Srivastava A. Activation of the NF-kappaB pathway by adeno-associated virus (AAV) vectors and its implications in immune response and gene therapy. Proc Natl Acad Sci U S A. 2011; 108:3743–3748. [PubMed: 21321191]
32. Kariko K, Ni H, Capodici J, Lamphier M, Weissman D. mRNA is an endogenous ligand for Toll-like receptor 3. J Biol Chem. 2004; 279:12542–12550. [PubMed: 14729660]
33. Zhang Z, Kim T, Bao M, Facchinetti V, Jung SY, Ghaffari AA, Qin J, et al. DDX1, DDX21, and DHX36 helicases form a complex with the adaptor molecule TRIF to sense dsRNA in dendritic cells. Immunity. 2011; 34:866–878. [PubMed: 21703541]
34. Tsai SY, Segovia JA, Chang TH, Morris IR, Berton MT, Tessier PA, Tardif MR, et al. DAMP molecule S100A9 acts as a molecular pattern to enhance inflammation during influenza A virus infection: role of DDX21-TRIF-TLR4-MyD88 pathway. PLoS Pathog. 2014; 10:e1003848. [PubMed: 24391503]
35. Tang Y, Bian Z, Zhao L, Liu Y, Liang S, Wang Q, Han X, et al. Interleukin-17 exacerbates hepatic steatosis and inflammation in non-alcoholic fatty liver disease. Clin Exp Immunol. 2011; 166:281–290. [PubMed: 21985374]
36. Li L, Chen L, Hu L, Liu Y, Sun HY, Tang J, Hou YJ, et al. Nuclear factor high-mobility group box1 mediating the activation of Toll-like receptor 4 signaling in hepatocytes in the early stage of nonalcoholic fatty liver disease in mice. Hepatology. 2011; 54:1620–1630. [PubMed: 21809356]
37. Affo S, Rodrigo-Torres D, Blaya D, Morales-Ibanez O, Coll M, Millan C, Altamirano J, et al. Chemokine Receptor Ccr6 Deficiency Alters Hepatic Inflammatory Cell Recruitment and Promotes Liver Inflammation and Fibrosis. PLoS One. 2015; 10:e0145147. [PubMed: 26691857]
38. Hammerich L, Bangen JM, Govaere O, Zimmermann HW, Gassler N, Huss S, Liedtke C, et al. Chemokine receptor CCR6-dependent accumulation of gammadelta T cells in injured liver restricts hepatic inflammation and fibrosis. Hepatology. 2014; 59:630–642. [PubMed: 23959575]
39. Roh YS, Zhang B, Loomba R, Seki E. TLR2 and TLR9 contribute to alcohol-mediated liver injury through induction of CXCL1 and neutrophil infiltration. Am J Physiol Gastrointest Liver Physiol. 2015; 309:G30–41. [PubMed: 25930080]
40. Saelens X, Festjens N, Parthoens E, Vanoverberghe I, Kalai M, van Kuppeveld F, Vandenabeele P. Protein synthesis persists during necrotic cell death. J Cell Biol. 2005; 168:545–551. [PubMed: 15699214]
41. Saito K, Dai Y, Ohtsuka K. Enhanced expression of heat shock proteins in gradually dying cells and their release from necrotically dead cells. Exp Cell Res. 2005; 310:229–236. [PubMed: 16129430]
42. Vanden Berghe T, Kalai M, Denecker G, Meeus A, Saelens X, Vandenabeele P. Necrosis is associated with IL-6 production but apoptosis is not. Cell Signal. 2006; 18:328–335. [PubMed: 16023831]
43. Cullen SP, Henry CM, Kearney CJ, Logue SE, Feoktistova M, Tynan GA, Lavelle EC, et al. Fas/CD95-induced chemokines can serve as “find-me” signals for apoptotic cells. Mol Cell. 2013; 49:1034–1048. [PubMed: 23434371]
44. Yatim N, Jusforgues-Saklani H, Orozco S, Schulz O, Barreira da Silva R, Reis Sousa C, Green DR, et al. RIPK1 and NF-kappaB signaling in dying cells determines cross-priming of CD8(+) T cells. Science. 2015; 350:328–334. [PubMed: 26405229]
45. Allen K, Jaeschke H, Copple BL. Bile acids induce inflammatory genes in hepatocytes: a novel mechanism of inflammation during obstructive cholestasis. Am J Pathol. 2011; 178:175–186. [PubMed: 21224055]
46. Brempelis KJ, Crispe IN. Infiltrating monocytes in liver injury and repair. Clin Transl Immunology. 2016; 5:e113. [PubMed: 27990288]
47. Mossanen JC, Krenkel O, Ergen C, Govaere O, Liepelt A, Puengel T, Heymann F, et al. Chemokine (C-C motif) receptor 2-positive monocytes aggravate the early phase of acetaminophen-induced acute liver injury. Hepatology. 2016; 64:1667–1682. [PubMed: 27302828]
48. Holt MP, Cheng L, Ju C. Identification and characterization of infiltrating macrophages in acetaminophen-induced liver injury. J Leukoc Biol. 2008; 84:1410–1421. [PubMed: 18713872]

49. Ramachandran P, Pellicoro A, Vernon MA, Boulter L, Aucott RL, Ali A, Hartland SN, et al. Differential Ly-6C expression identifies the recruited macrophage phenotype, which orchestrates the regression of murine liver fibrosis. Proc Natl Acad Sci U S A. 2012; 109:E3186–3195. [PubMed: 23100531]

50. Dal-Secco D, Wang J, Zeng Z, Kolaczkowska E, Wong CH, Petri B, Ransohoff RM, et al. A dynamic spectrum of monocytes arising from the in situ reprogramming of CCR2+ monocytes at a site of sterile injury. J Exp Med. 2015; 212:447–456. [PubMed: 25800956]

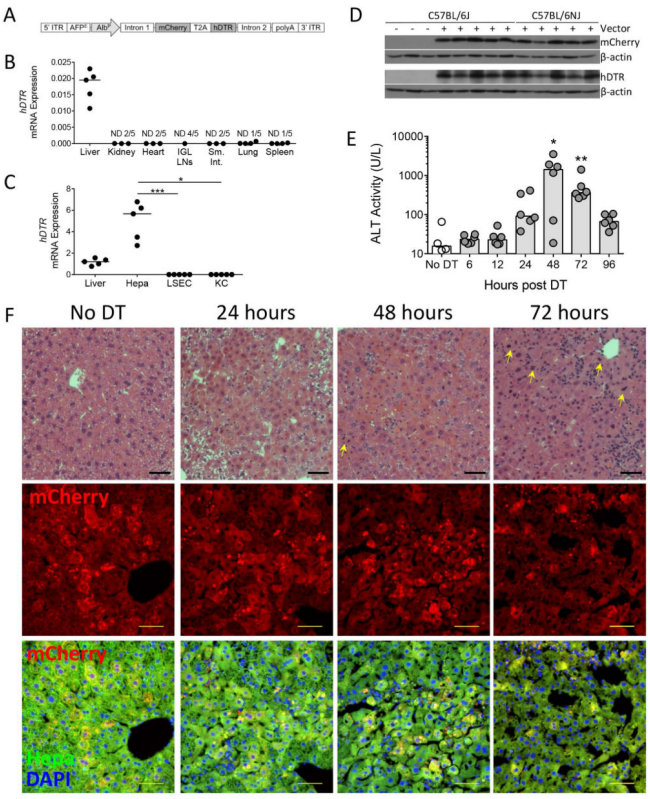

Figure 1. Hepatocyte-specific expression of rAAV8.pAlb.mCherry.hDTR results in peak liver damage 48 hours following DT injection

(A) rAAV8.pAlb.mCherry.hDTR vector encoding the mouse AFP^E and Alb^P; mCherry and the hDTR linked by a T2A linker sequence; and AAV serotype-2 5′ and 3′ ITRs. Two weeks following rAAV injection, mice received either no injection, 1X PBS (control), or DT and were sacrificed 6, 12, 24, 48, 72, or 96 hours later. *hDTR* mRNA levels, relative to (B) *Gapdh* in organs and (C) *Hprt* in total liver and liver cell populations of C57BL/6NJ mice that received 1X PBS, each data point represents an individual mouse (n = 5). (D) Western blot detection of mCherry, hDTR, and β-actin in the hepatocytes of C57BL/6J mice that did not receive rAAV and in C57BL/6J and C57BL/6NJ mice that received rAAV and 1X PBS. (E) Serum ALT levels in C57BL/6J mice that received no DT or DT. Each data point represents an individual mouse, bars represent the median. (F, top row) Paraffin-embedded sections stained for hematoxylin and eosin, 100X. Bar, 50 μm. Arrow, mitotic hepatocytes. (F, middle and bottom rows) Cryo-preserved sections with mCherry (top) or the merge of mCherry fluorescence (red), hepatocyte autofluorescence (green), and DAPI to distinguish nuclei (blue) (bottom). Bar, 50 μm. (D–F) are combined from two experiments (n = 4–6 per group). Representative images chosen from one mouse at each time point for (F), based on median ALT levels. Significance determined by a Kruskal-Wallis test followed by Dunn's post-test (C) of Liver, LSEC, and KC to hepatocytes and (E) of each time point to the No DT group median. * represents significance compared to No DT group; *, $P \leq 0.05$; **, $P \leq 0.01$; ***, $P \leq 0.001$; non-significance represented by absence of bar or asterisk. AFP^E, AFP enhancer; Alb^P, albumin promoter; DAPI, 4′,6-diamidino-2-phenylindole; DT, diphtheria toxin; Hepa; hepatocyte; hDTR, human diphtheria toxin receptor; ITR, inverted terminal

repeats; IGL, inguinal lymph nodes; KC, Kupffer cell; LSEC, liver sinusoidal endothelial cell; Sm. Int., small intestine; and ND, non-detect.

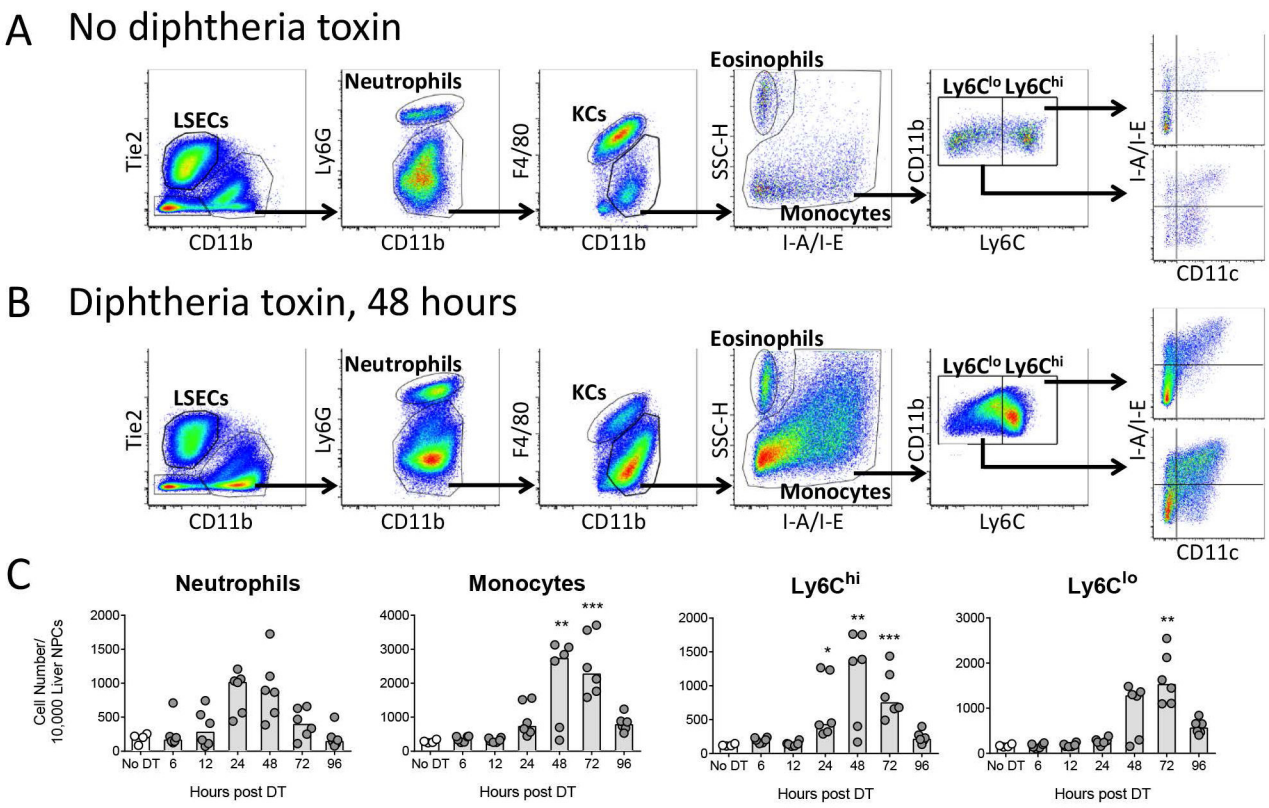

Figure 2. Hepatocyte death promotes the infiltration of neutrophils and monocytes

Two weeks following rAAV injection, C57BL/6J mice received DT and were sacrificed 6, 12, 24, 48, 72, or 96 hours later. Representative gating scheme to identify cell populations within the liver of (A) control mice and (B) DT-treated mice 48 hours after DT injection. (C) Neutrophil, monocyte, Ly6C^{hi} monocyte, and Ly6C^{lo} monocyte cell numbers. (A–C) Data are combined from two experiments, each data point represents an individual mouse (n = 4–6 per group), bars represent the median. (C) Significance determined by a Kruskal-Wallis test followed by Dunn's post-test of each time point to the No DT group. * represents significance compared to No DT group; *, $P \leq 0.05$; **, $P \leq 0.01$; ***, $P \leq 0.001$; non-significance represented by absence of asterisk. DT, diphtheria toxin; KC, Kupffer cell; and LSEC, liver sinusoidal endothelial cell.

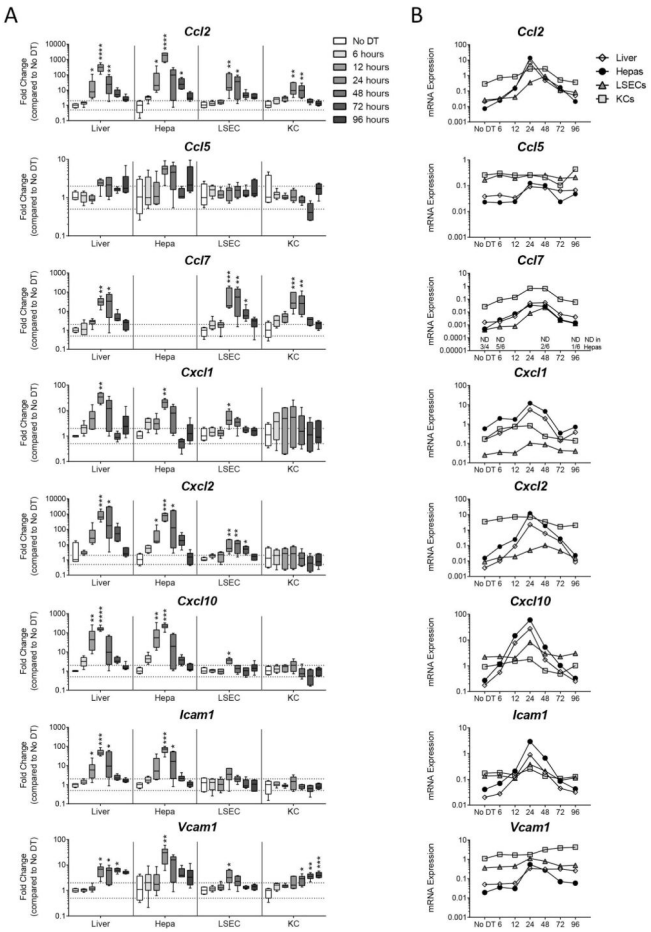

Figure 3. Hepatocyte death up-regulates genes associated with myeloid cell recruitment, predominantly in hepatocytes

Two weeks following rAAV injection, C57BL/6J mice received DT and were sacrificed 6, 12, 24, 48, 72, or 96 hours later. (A) Fold change gene expression in total liver, hepatocytes, LSECs, and KCs compared to the No DT group median, *Hprt* used as reference gene. Data are median and range. (B) mRNA expression relative to *Hprt* in total liver, hepatocytes, LSECs, and KCs. Median values only represented. For *Ccl7*, non-detect values represented on graph are for hepatocyte population only. (A, B) Data are combined from two experiments, each data point represents an individual mouse (n = 4–6 per group). (A) Significance determined by a Kruskal-Wallis test followed by Dunn's post-test of each time point to the No DT group. * represents significance compared to No Dt group; *, $P \leq 0.05$; **, $P \leq 0.01$; ***, $P \leq 0.001$; ****, $P \leq 0.0001$; non-significance represented by absence of asterisk. DT, diphtheria toxin; Hepa, hepatocyte; KC, Kupffer cell; and LSEC, liver sinusoidal endothelial cell; and ND, non-detect.

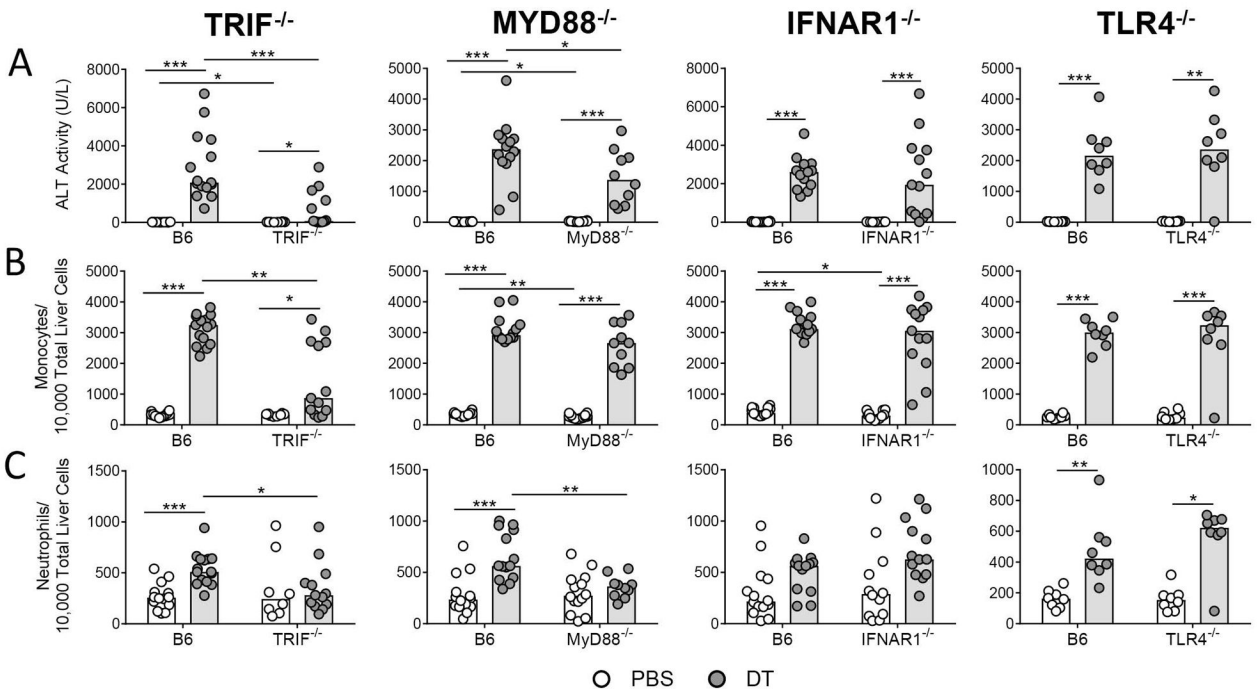

Figure 4. TRIF$^{-/-}$ mice exhibit less inflammation than MyD88$^{-/-}$, IFNAR1$^{-/-}$, and TLR4$^{-/-}$ mice following hepatocyte death

(A) Serum ALT levels, (B) monocyte, and (C) neutrophil numbers in rAAV-transduced C57BL/6J, TRIF$^{-/-}$, MyD88$^{-/-}$, IFNAR1$^{-/-}$, and TLR4$^{-/-}$ mice 48 hours following injection of 1X PBS or DT. Data are combined for 3 independent TRIF$^{-/-}$ experiments, 3 independent MyD88$^{-/-}$ experiments, 3 independent IFNAR1$^{-/-}$ experiments, and 2 independent TLR4$^{-/-}$experiments. The B6 mice used in the third repetition of the IFNAR1$^{-/-}$ experiments were also used for the third repetition of the MyD88$^{-/-}$ experiments, so the data appears twice (n = 4, B6 + PBS and B6 + DT groups). Each data point represents an individual mouse (n = 8–15 per group), bars represent the median. Significance determined by four pairwise Mann-Whitney tests and the p-values adjusted for multiple comparisons using the Holm-Bonferroni method as described in the methods. *, $P \leq 0.05$; **, $P \leq 0.01$; ***, $P \leq 0.001$; non-significance represented by absence of bar. DT, diphtheria toxin; TRIF, TIR-domain-containing adapter-inducing interferon-β; MyD88, myeloid differentiation primary-response protein 88, IFNAR, IFN (α and β) receptor 1; and TLR4, Toll-like receptor 4.

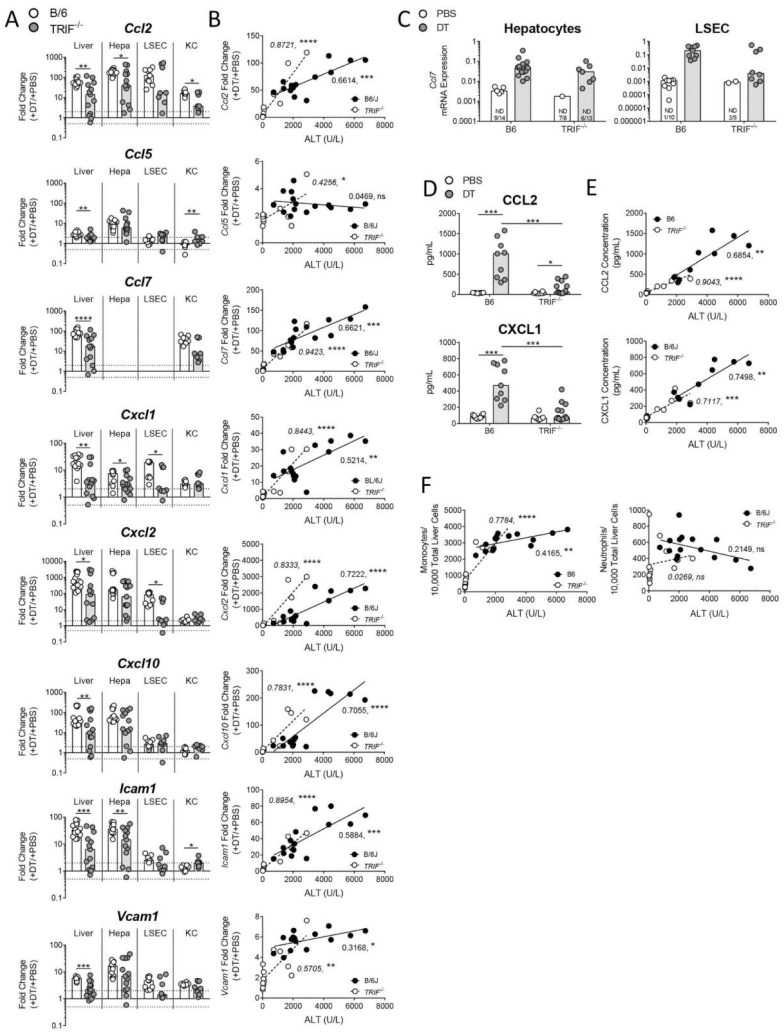

Figure 5. Absence of TRIF results in reduced production of myeloid cell-recruiting factors, except in mice exhibiting breakthrough inflammation

Two weeks following rAAV injection, C57BL/6J and TRIF$^{-/-}$ mice received PBS or DT and were sacrificed 48 hours later. (A) Fold change gene expression in total liver, hepatocytes, LSECs, and KCs, + PBS group and + DT group compared to the + PBS group median, *Hprt* was used as the reference gene. (C) mRNA expression relative to *Hprt* for *Ccl7* in hepatocytes and LSECs as non-detects in the + PBS groups complicated fold change calculations. (D) Serum protein levels for CCL2 and CXCL1. Correlation of serum ALT with (B) gene expression fold change levels in total liver, (E) serum chemokines, and (F) monocyte and neutrophil infiltrate for B6 + DT (black) and TRIF$^{-/-}$ + DT (white) groups. (A–G) Data are combined for 2–3 experiments. Each data point represents an individual mouse, bars represent the median. For (A–C, F) total liver and hepatocytes n = 8–15 per group and for LSECs and KCs n = 5–10 per group. For (D, E) serum: n = 10, B6 + PBS; n = 9, B6 + DT; n = 8, TRIF$^{-/-}$ + PBS; n = 13, TRIF$^{-/-}$ + DT. (A) *Ccl2* has one non-detect value in each + PBS group not noted on the graph. Significance determined by (A) an individual Mann-Whitney test per population, (B, E, F) Goodness of Fit, with R^2 and p-value reported on the graph, and (D) by four pairwise Mann-Whitney tests and the p-values adjusted for

multiple comparisons using the Holm-Bonferroni method as described in the methods. *, $P \leq 0.05$; **, $P \leq 0.01$; ***, $P \leq 0.001$; ****, $P \leq 0.0001$; non-significance represented by absence of bar. B6, C57BL/6J; DT, diphtheria toxin; Hepa; hepatocyte; KC, Kupffer cell; LSEC, liver sinusoidal endothelial cell; TRIF, TIR-domain-containing adapter-inducing interferon-β; MyD88, myeloid differentiation primary-response protein 88; and ND, non-detect.

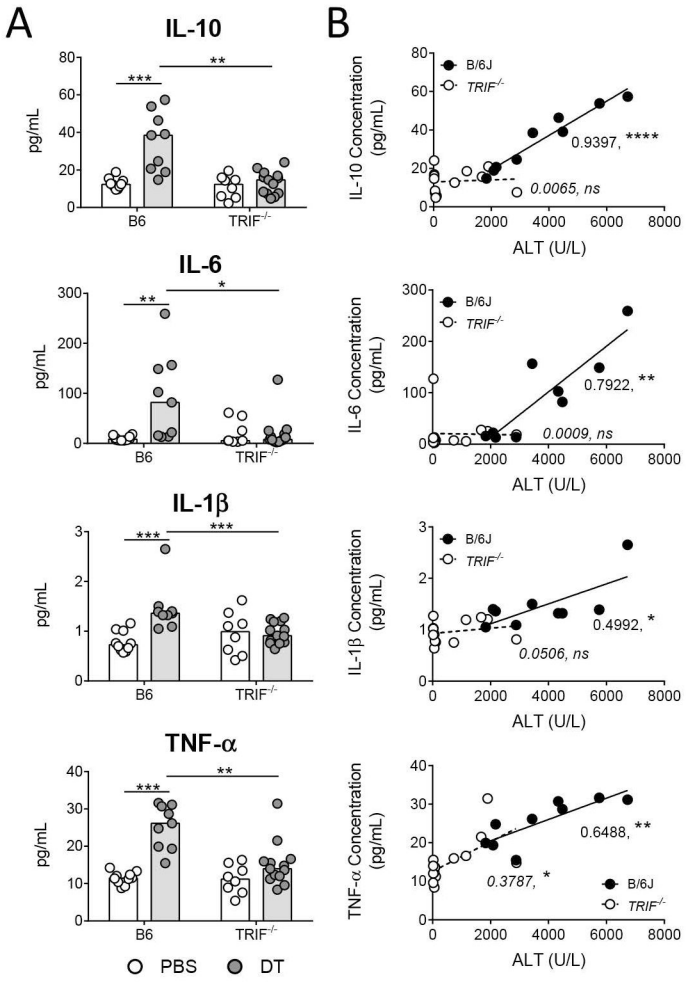

Figure 6. Increased production of IL-10, IL-6, and IL-1β depends on TRIF

(A) Serum chemokine levels in rAAV-transduced C57BL/6J and TRIF$^{-/-}$ mice 48 hours following injection of 1X PBS or DT. (B) Correlation of serum ALT levels with gene expression fold change levels for B6 + DT (black) and TRIF$^{-/-}$ + DT (white) groups. Data are combined for 2–3 independent experiments. Each data point represents an individual mouse (n = 8–13 per group), bars represent the median. Significance determined by (A) four pairwise Mann-Whitney tests and the p-values adjusted for multiple comparisons using the Holm-Bonferroni method as described in the methods and (B) Goodness of Fit, with R^2 and p-value reported on the graph. *, P ≤ 0.05; **, P ≤ 0.01; ***, P ≤ 0. 001; ****, P ≤ 0.0001; non-significance represented by absence of bar. B6, C57BL/6J; DT, diphtheria toxin; and TRIF, TIR-domain-containing adapter-inducing interferon-β.

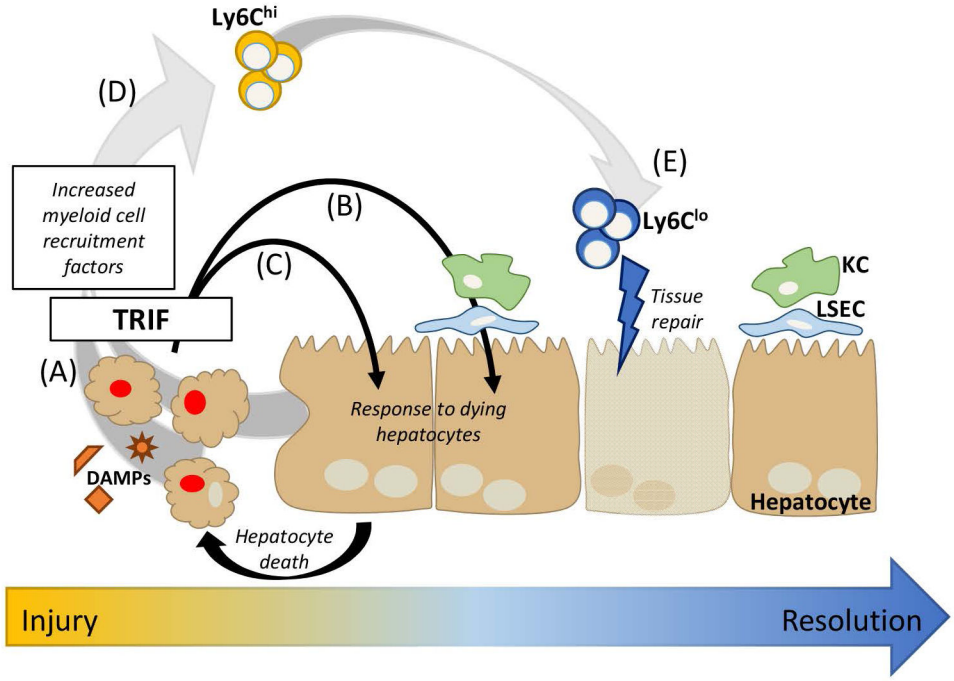

Figure 7. Model of TRIF-mediated signaling following hepatocyte death

Following hepatocyte death, there are multiple mechanisms by which inflammation may be propagated in the liver via TRIF signaling pathways. (A) Dying hepatocytes may themselves up-regulate inflammatory transcripts, (B) neighboring, live hepatocytes may up-regulate inflammatory transcripts in response to inflammatory mediators produced by LSECs or KCs or by dying hepatocytes, or (C) DAMPs and other inflammatory mediators released by dying hepatocytes may induce the death of neighboring hepatocytes, propagating the cycle of death and inflammation. (D) The production of myeloid cell recruitment factors by dying hepatocytes, live hepatocytes, and/or other liver cells results in Ly6C^{hi} monocyte infiltration which may (E) differentiate into Ly6C^{lo} monocyte-derived macrophages that likely aid in tissue repair. DAMPs; damage-associated molecular patterns; KC, Kupffer cell; LSEC, liver sinusoidal endothelial cell; and TRIF, TIR-domain-containing adapter-inducing interferon-β.